THERMO-MECHANICAL PROCESS MODELLING OF INDUSTRIALLY PULTRUDED PARTS HAVING UD AND CFM LAYERS

Ismet Baran*[1], Jesper H. Hattel[1], Remko Akkerman[2]

[1] *Technical University of Denmark, Mechanical Engineering Department, 2800 Kgs. Lyngby, Denmark*
[2] *University of Twente, Faculty of Engineering Technology, NL-7500AE Enschede, The Netherlands*
* *Corresponding Author: isbar@mek.dtu.dk*

Keywords: Pultrusion, Warpage, Residual stresses, Curing, Computational modelling.

Abstract
Numerical process simulation of an industrially pultruded rectangular hollow profile is presented. The product contains the continuous filament mat (CFM) and the uni-directional(UD) roving layers made of glass/polyester. The distortion and stress evolutions together with the temperature and degree of fields are predicted by the simulation tool developed by the authors. The predicted deformation pattern at the end of the process is found to agree quite well with the one for the real pultruded part in a commercial pultrusion company. A parametric study is also performed based on the total volumetric shrinkage of the resin system during curing. The process induced residual stresses are calculated in the in-plane directions which have the potential to influence the internal stress levels during the service loading conditions.

1. Introduction

Pultrusion process is one of the most effective manufacturing techniques for production of composite materials having constant cross-sectional area. Pultruded composite profiles are getting increasingly popular in construction industry as well as in wind energy due to their high strength-to-weight ratio, low maintenance cost and high corrosion resistance.A schematic view of a pultrusion process is shown in Fig. 1. The reinforcements in the form of continuous unidirectional (UD) roving or continuous filament mats (CFM) are held on creel racks and fed continuously through a guiding system. These reinforcements are impregnated with the desired matrix system in a resin bath. The wetted-out reinforcement pack is then collimated into a preformed shape before entering the heating die. A polymerization takes place inside the die with the help of the heat coming from the heaters. The cured profile is advanced via a pulling system to the cut-off saw where the finished product is cut to desired lengths. Recently, pultruded profiles are foreseen to have potential for the replacement of some of the conventional materials used in the construction industry. An example of this is the increased application of structural pultruded profiles for bridge constructions. Therefore, in order to increase the product quality and the degree of reliability of the pultruded products, a series of processing design challenges must be tackled such as process induced residual stresses and distortions. Industrially pultruded parts generally contain the combination of UD roving with CFM layers which have different thermal and mechanical properties, i.e. the former has transversely isotropic properties, and on

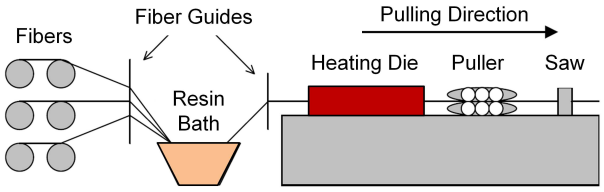

Figure 1. Schematic view of a pultrusion process.

the other hand the latter has the quasi-isotropic properties. At present, no contribution has been given in the literature regarding the thermo-chemical-mechanical behaviour of the industrially pultruded products during processing.

In literature, several numerical and experimental analyses have been carried out for the pultrusion process [1–11]. Of these studies, the pulling force [1, 2], the temperature and degree of cure developments [3–7], the process induced residual stresses and distortions [8] have been investigated. In addition, probabilistic modelling of the pultrusion has been proposed in [9] and process optimization studies have been carried out in [10, 11].

A novel thermo-chemical-mechanical analysis of the pultrusion process is carried out in the present work. A process simulation is performed for an industrially pultruded rectangular hollow profile containing both UD roving and CFM layers. The reinforcements are impregnated with a commercial polyester resin mixture (Atlac 382 [12]). The reactivity of the resin is obtained from gel tests performed by the pultruder. The cure kinetics parameters are estimated from a fitting procedure against the measured temperature. Two different micromechanics approaches are used to calculate the instantaneous mechanical properties of the UD and the CFM layers.

2. Numerical Implementation

Temperature and degree of cure distributions at steady state are calculated in the 3D thermo-chemical analysis. The energy equations given in Eq. 1, Eq. 2 and Eq. 3 are solved for the UD layer, the CFM layer and the heating die, respectively in a commercial finite element software ABAQUS [13]. Here, x_1 is the pulling or longitudinal direction; x_2 and x_3 are the transverse directions for the UD layer. On the other hand, x_1 (pulling direction) and x_2 are the in-plane directions and x_3 is the out-of-plane direction for the CFM layer.

$$(\rho C_p)_{UD}\left(u\frac{\partial T}{\partial x_1}\right) = k_{x_1,UD}\frac{\partial^2 T}{\partial x_1^2} + k_{x_2,UD}\frac{\partial^2 T}{\partial x_2^2} + k_{x_3,UD}\frac{\partial^2 T}{\partial x_3^2} + q_{UD} \tag{1}$$

$$(\rho C_p)_{CFM}\left(u\frac{\partial T}{\partial x_1}\right) = k_{x_1,CFM}\frac{\partial^2 T}{\partial x_1^2} + k_{x_2,CFM}\frac{\partial^2 T}{\partial x_2^2} + k_{x_3,CFM}\frac{\partial^2 T}{\partial x_3^2} + q_{CFM} \tag{2}$$

$$0 = k_{x_1,d}\frac{\partial^2 T}{\partial x_1^2} + k_{x_2,d}\frac{\partial^2 T}{\partial x_2^2} + k_{x_3,d}\frac{\partial^2 T}{\partial x_3^2} \tag{3}$$

where T is the temperature, u is the pulling speed, ρ is the density, C_p is the specific heat and k_{x_1}, k_{x_2} and k_{x_3} are the thermal conductivities along x_1-, x_2- and x_3-directions, respectively. The

subscripts UD, CFM and d correspond to the UD layer, the CFM layer and the die, respectively. Lumped material properties are used and assumed to be constant. The source term q in Eq. 1 and Eq. 2 are related to the internal heat generation due to the exothermic reaction of the polyester resin and expressed as:

$$q_{UD} = (1 - V_f)_{UD}\rho_r H_{tr} R_r(\alpha, T) \tag{4}$$

$$q_{CFM} = (1 - V_f)_{CFM}\rho_r H_{tr} R_r(\alpha, T) \tag{5}$$

where H_{tr} is the total heat of reaction for the polyester during the exothermic reaction, ρ_r is the resin density, V_f is the fiber volume fraction, α is the degree of cure, and $R_r(\alpha, T)$ is the reaction of cure which can also be defined as the rate of α, i.e. $d\alpha/dt$. The expression for the cure kinetics is given as:

$$R_r(\alpha, T) = \frac{d\alpha}{dt} = A_0 \exp(\frac{-E_a}{RT})\alpha^m(1 - \alpha)^n \tag{6}$$

where A_0 is the pre-exponential constant, E_a is the activation energy, R is the universal gas constant, m and n are the order of reaction (kinetic exponents). The relation of the resin kinetics equation for the steady state approach can be expressed as [8]

$$0 = R_r(\alpha, T) - u\frac{\partial \alpha}{\partial x_1} \tag{7}$$

which is used in the 3D steady state thermo-chemical model.

In the 2D quasi-static mechanical model, the elastic modulus of the resin is modelled using the cure hardening instantaneous linear elastic (CHILE) approach proposed by Johnston [14]. The effective mechanical properties of the UD layer are calculated using the self consistent field micromechanics (SCFM) approach which is a well known and documented technique in the literature [15]. On the other hand, the effective mechanical properties of the quasi-isotropic CFM layer is calculated considering the material properties of the UD layer obtained by the SCFM approach for the same V_f as the quasi-isotropic layer [16]. The details of the calculations for a quasi-isotropic laminate are provided by Akkerman [16]. An incremental linear elastic approach is implemented utilizing the user defined subroutines in ABAQUS to calculate the displacements and stresses.

3. Model Description

The 3D thermo-chemical analysis implemented in ABAQUS is used to simulate the pultrusion process of a rectangular hollow profile. A glass/polyester is considered for the UD and the CFM layers and steel is used for the die. The details of the process set-up is taken from a commercial pultrusion company. A schematic representation of the model is seen in Fig. 2. Only a quarter model is used due to symmetry conditions. The 3D thermo-chemical model is subsequently coupled with a 2D quasi-static mechanical model in which quadratic generalized plane strain elements are utilized in ABAQUS. The cross sectional details including the meshing are given in Fig. 3. It is seen that the dimension of the processing hollow rectangular profile is 64×27×3 mm. A local material orientation is employed for the CFM layer as seen in Fig. 3 in order to reflect the in-plane (x_1- and x_2-direction) and the out-of-plane (x_3-direction) properties

correctly. For the round corner, a cylindrical local coordinate system is used in which the x_2- and x_3-directions are taken as the tangential (T) and radial (R) directions, respectively. The die and the mandrel are also included in the 2D mechanical model (see Fig. 3) in which a mechanical contact formulation is defined at the die-part and mandrel-part interface. By using this contact formulation, a separation due to the thermal contraction of the part and/or the resin shrinkage at the interface is allowed and any expansion of the composite beyond the tool interfaces is restricted. The friction force at the contact surfaces is assumed to be zero (sliding condition). Symmetry mechanical BCs are applied at the symmetry lines and the die is assumed to be fixed at the outer regions as shown in Fig. 3.

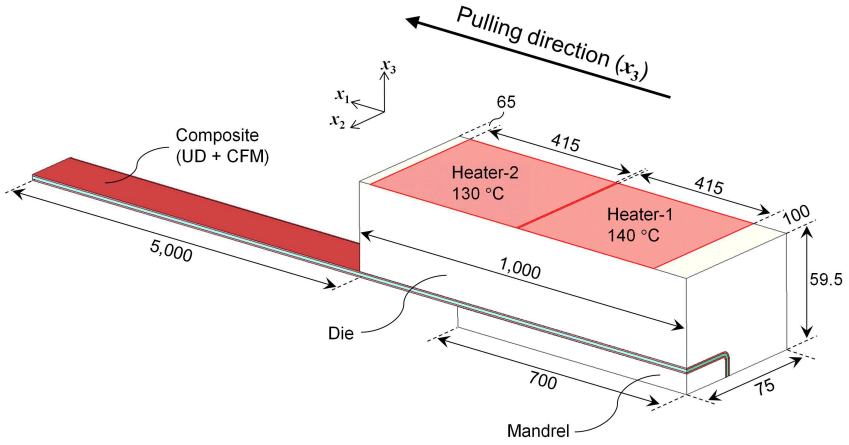

Figure 2. Schematic view of the quarter pultrusion domain for the pultruded rectangular hollow profile. All dimensions are in mm.

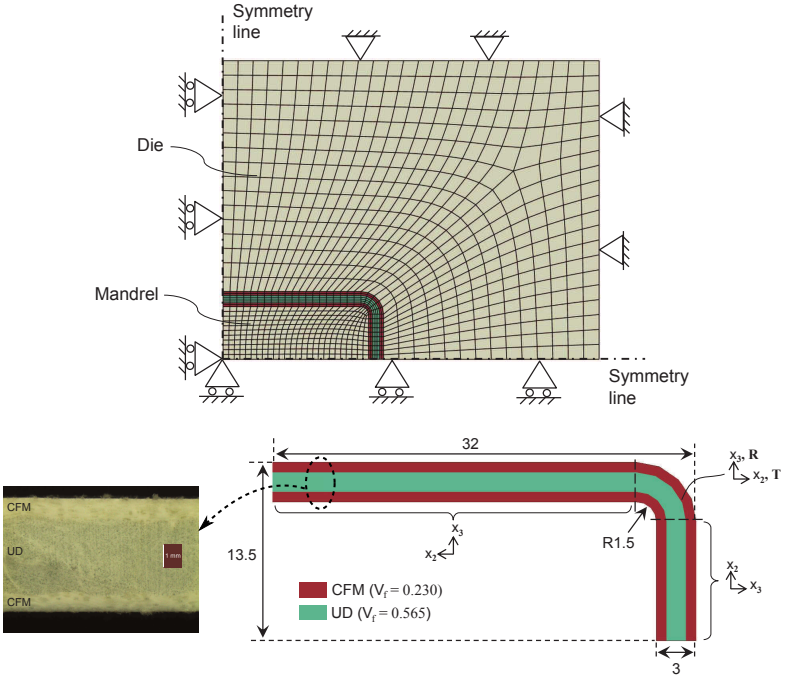

Figure 3. The cross sectional details of the pultruded profile, die and mandrel used in the pultrusion process model. All dimensions are in mm.

4. Results and Discussions

The predicted vertical displacement development for point A (die-part interface) in the x_3-direction is depicted in Fig. 4 for various total volumetric shrinkage values (V_{sh} = 0.02, 0.04, 0.06, 0.08, 0.10 and 0.12). The trend of the displacement development is found to be almost the same for different V_{sh} values. However, the magnitude of the displacement decreases with a decrease in V_{sh} which is expected. The detachment at the die-part interface is captured using the mechanical contact formulation at the interface as seen from Fig. 4. The part separates from the die due to the chemical shrinkage. The detachment point where the displacement starts being negative shifts left towards the die inlet as the V_{sh} increases.

The deformed contour plots in Fig. 5 shows the predicted displacement field in the x_3-direction for V_{sh} values of 0.02, 0.06 and 0.10 at the end of the process. The deformation or warpage pattern is found to be almost the same for various V_{sh} values, however the magnitudes are different as aforementioned. The predicted warpage patterns (Fig. 5) match well with the warpage observed in the real pultruded rectangular hollow products seen in Fig. 5(*right*). The magnitude of the warpage (w) at point A is defined as the difference between the magnitude of the displacements at point A (w_a) and point C (w_c) seen in Fig. 5($left$), i.e. $w = w_a - w_c$. The warpage magnitudes of the pultruded products are also measured at the room temperature. The predicted and the measured warpage values are given in Table 1. A good agreement is found between the predicted and the measured values such that the predicted warpage value for V_{sh} of 0.10 and 0.12 are in the range of measured values.

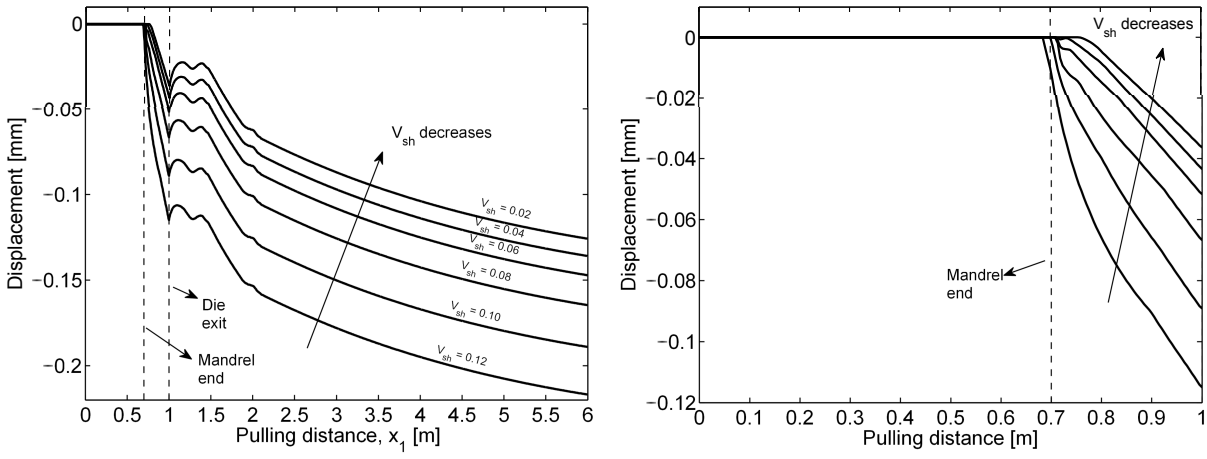

Figure 4. The displacement evolution at point A (die part interface) in the x_3-direction ($left$) and the corresponding zoomed plot inside the die (0-1 m) (*right*) for various V_{sh} values.

The predicted process induced residual stresses are shown in Fig. 6 as undeformed contour plots in the global material orientations in the x_2-x_3 plane. Here, S_{22} and $S_{33}$are the normal stresses in the x_2-, x_3-directions, respectively, and S23 is the in-plane shear stress. The magnitude of the maximum tension and compression for the normal stresses are calculated approximately as 10 MPa and 15 MPa, respectively. Stress concentration is found for S_{23} at the round corner of the product. It is seen that there is a discontinuity in the stress at the UD-CFM interface.

Table 1. The predicted and measured values for the warpage defined as $w = w_A - w_C$ (see Fig. 5).

	Predicted [mm]			**Measured** [mm]
	w_A	w_C	Warpage ($w = w_A - w_C$)	Warpage ($w = w_A - w_C$)
$V_{sh} = 0.02$	0.101	0.049	0.052	
$V_{sh} = 0.04$	0.111	0.051	0.060	
$V_{sh} = 0.06$	0.122	0.052	0.070	0.15 ± 0.05
$V_{sh} = 0.08$	0.140	0.053	0.087	
$V_{sh} = 0.10$	0.164	0.061	0.103	
$V_{sh} = 0.12$	0.192	0.075	0.117	

The proposed numerical simulation for the thermo-chemical-mechanical analysis of the pultrusion process has a great potential for the future investigation of the residual stresses and shape distortions for more complex pultruded profiles. More specifically, the distortions might be important for rigid polymer structures such as window frames and fencing panels due to their desired high geometrical precision. The residual stresses would have an important effect on the mechanical behaviour of the pultruded structural profiles such as wind turbine blade and I-beam (especially at the web-flange junction (WFJ)) since residual stresses have the potential to influence the internal stress levels arise in the pultruded products. Therefore, the residual stresses and shape distortions arise in the pultrusion process have to be analysed carefully.

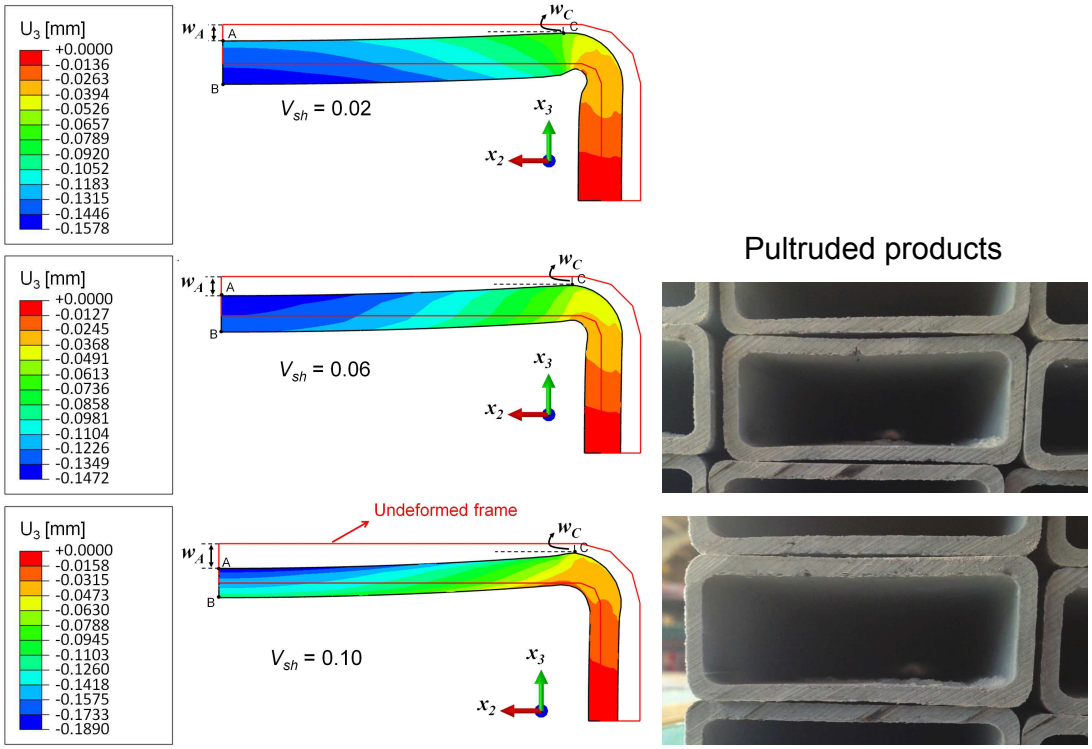

Figure 5. Deformed contour plots of the residual displacement field in the x_3-direction and the initial geometry of the cross section (undeformed frame) (*left*). Scale factor for the deformed shape is 10. The warpage formation observed in the real pultruded hollow rectangular profiles (*right*).

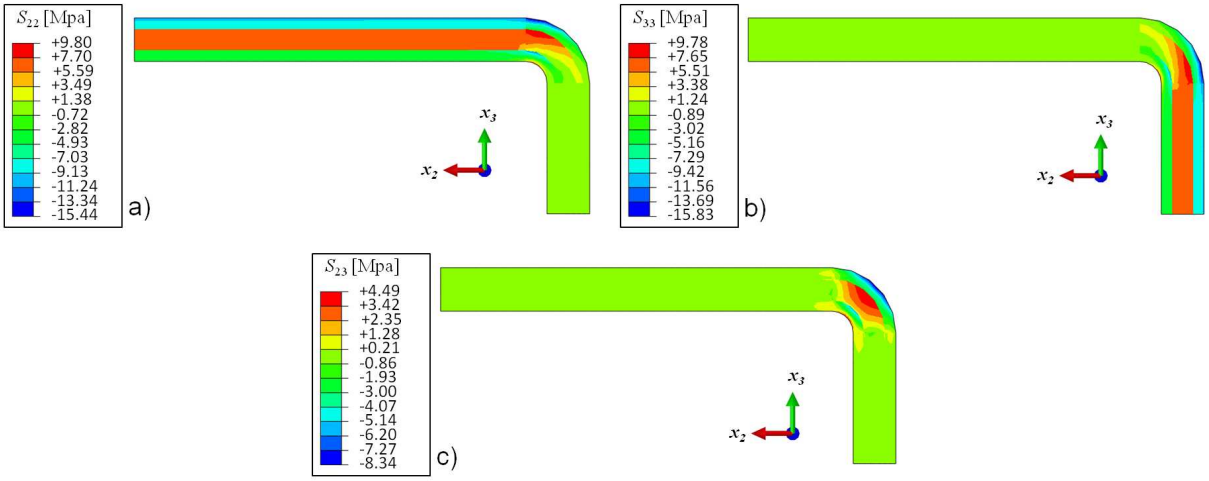

Figure 6. Contour plots showing the in-plane normal stresses S_{22} (a) and S_{33} (b) in the x_2 and x_3 directions, respectively, and the in-plane shear stress S_{23} (c).

5. Conclusions

In the present work, thermo-chemical-mechanical analysis of the pultrusion of a rectangular hollow profiles was performed using the FEM. A glass/polyester composite was considered for the UD and the CFM layers. The resin cure kinetics are obtained from the gel tests performed by the pultruder. The warpage formation at the end of the process was predicted and the warpage pattern was found to agree well with the warpage observed in a real industrially pultruded products. Moreover, the in-plane residual stresses over the cross section of the pultruded part are calculated and a stress discontinuity is found at the UD-CFM interface. The through-thickness stress variations may decrease the quality of bonding between the UD and CFM layers. In addition, the failure modes as well as the delamination resistance may also be affected by the through-thickness stress variations.

References

[1] S.M. Moschiar, M.M. Reboredo, H. Larrondo, A. Vazquez. Pultrusion of epoxy matrix composites: pulling force model and thermal stress analysis. *Polymer Composites*,17(6):850-858,1996.

[2] P. Carlone, I. Baran, J.H. Hattel, G.S. Palazzo. Computational Approaches for Modeling the Multiphysics in Pultrusion Process. *Advances in Mechanical Engineering*, vol. 2013, Article ID 301875, 14 pages, 2013, doi:10.1155/2013/301875.

[3] M. Valliappan, J.A. Roux, J.G. Vaughan, E.S. Arafat. Die and post-die temperature and cure in graphite-epoxy composites. *Compos Part B: Eng*, 27:1-9,1996.

[4] Y.R. Chachad, J.A. Roux, J.G. Vaughan, E. Arafat. Three-dimensional characterization of pultruded fiberglass-epoxy composite materials. *J Reinf Plast Comp*,14:495-512,1995.

[5] I. Baran, J.H. Hattel, C.C. Tutum. Thermo-Chemical Modelling Strategies for the Pultrusion Process. *App Compos Mat.*, 20(6):1247-1263,2013.

[6] I. Baran, C.C. Tutum, J.H. Hattel. The effect of thermal contact resistance on the thermosetting pultrusion process. *Compos Part B: Eng*, 45:995-1000,2013.

[7] P. Carlone, G.S. Palazzo, R. Pasquino. Pultrusion manufacturing process development by computational modelling and methods. *Math Comput Model*, 44:701-709,2006.

[8] I. Baran, C.C. Tutum, M.W. Nielsen, J.H. Hattel. Process induced residual stresses and distortions in pultrusion. *Compos Part B: Eng*, 51:148-161,2013.

[9] I. Baran, C.C. Tutum, J.H. Hattel. Reliability estimation of the pultrusion process using the first-order reliability method (FORM). *App Compos Mat.*, 20:639-653,2012.

[10] I. Baran, C.C. Tutum, J.H. Hattel. Optimization of the thermosetting pultrusion process by using hybrid and mixed integer genetic algorithms. *App Compos Mat.*, 20:449-463,2012.

[11] P. Carlone, G.S. Palazzo. Pultrusion manufacturing process development: Cure optimization by hybrid computational methods. *Comput. Math. Appl.*, 53:1464-1471,2007.

[12] Atlac 382 Technical Data Sheet, DSM Composite Resins (2003).

[13] ABAQUS 6.11 Reference Guide. Dassault Systems (2011).

[14] A. Johnston. *An Integrated Model of the Development of Process-Induced Deformation in Autoclave Processing of Composites Structures*, Ph.D. thesis, The University of British Columbia, Vancouver, 1997.

[15] T.A. Bogetti, J.W. Jr Gillespie. Process-induced stress and deformation in thick-section thermoset composite laminates. *J Compos Mater*, 26(5):626-660,1992.

[16] R. Akkerman. On the properties of quasi-isotropic laminates. *Compos part B: Eng*, 33:133-140,2002.